Pre-swirl energy saving device in marine application

IOP Conf. Series: Journal of Physics: Conf. Series **1101** (2018) 012015 doi:10.1088/1742-6596/1101/1/012015

Pre-swirl energy saving device in marine application

P Król[1,2] and K Tesch[1]

[1]Faculty of Mechanical Engineering, Gdańsk University of Technology, Gdańsk, Poland
[2]Ship Design and Research Centre, Gdańsk, Poland

E-mail: przemyslaw.krol@cto.gda.pl

Abstract. This paper covers topics of energy saving device (ESD) with application to marine propulsors. The form of ESD, considered in this paper, consists of fixed lifting foils mounted in front of the screw propeller (the pre-swirl stator/guide vanes). An algorithm for designing propulsion systems, consisting of guide vanes and screw propeller, is presented. The proposed method relies on hybrid lifting line (guide vanes)-lifting surface (screw propeller) vortex model. Additionally, an analysis method for such systems is also presented. It utilises lifting surface model for guide vanes as well as for screw propeller blades. Accuracy of the proposed method is notably lower in comparison with CFD calculations, however, the former is substantially faster and at the same time capable of providing accuracy sufficient for practical application. Further, the entire process of design and analysis is presented on the example of Nawigator XXI ship. The designed propulsion system, consisting of propeller CP753 and pre-swirl stator ST002, was manufactured and tested in model scale. Model tests revealed increased efficiency by 4% in the design point in comparison with with the Nawigator's original propeller CP469. Finaly, model scale experimental results, conducted in Ship Hydrodynamics Division of CTO Gdańsk, are compared with numerical predictions.

1. Introduction

The pre-swirl stator is an energy saving device in the form of fixed stator blades mounted in front of the operating propeller. ESD are widely applied in the field of energy generation industry, however, their application in marine propulsion systems is rather limited. Although such devices are known in the literature [11], modern design methods of pre-swirl stators involve multiple CFD calculations of subsequent configurations [8, 9, 11]. Methods based on inviscid flow theory are much faster but at the same time they are less accurate than CFD [4, 11]. However, carefully conducted inviscid calculations are even capable of realistic reproduction of unsteady cavitation phenomena [1]. Such a method would find an immediate practical application if it were thoroughly verified.

The vortex lattice method for designing propeller-pre-swirl stator systems was developed in CTO Gdańsk [5, 6]. This paper presents its improved version and its application. The propeller-stator system was designed for Nawigator XXI ship by means of the hybrid lifting line-lifting surface algorithm and analysed both numerically (lifting surface model CFD) and experimentally.

The discussed method takes advantage of the lifting line-lifting surface hybrid approach within the design-analysis loop. Despite simplicity of the adopted model, main characteristics of velocity fields are reproduced correctly. This is because an iterative procedure for relaxing free vortices shedding from the propeller and stator blades is applied. The geometry of free

vortices segments is rearranged in each time step in such way to satisfy force free condition on free vortex filaments [2]. Convergence is usually achieved after less than 20 iterations. This approach makes it possible to obtain reliable results with reasonable effort and time. There is no need for extensive computational power.

2. Practical application

The propulsion system consisting of controllable pitch propeller CP753 and pre-swirl stator ST002 was designed for Nawigator XXI vessel. Nawigator XXI was chosen because it was subject to numerous tests and a variety of full scale data is available. The original propulsion system consists of the controllable pitch propeller CP469 operating at constant RPM without any stator. Standard towing tank model tests were carried out in CTO Ship Hydromechanics Division. Open water characteristics for both propellers were determined – stator ST002 was not included in these tests as it was regarded as the hull appendage. Subsequently, self-propulsion tests with CP469, CP753 and with CP753+ST002 propulsors were conducted. This made it possible to confirm the main theoretical conclusions on stator's influence mechanism and operating features. Full scale power and rotational speed prediction indicate that the new propulsion system will increase efficiency by 4% in the design point. This can be considered as significant progress, since in case of huge marine engines reducing the demanded power even by a single percent leads to notable energy saving.

2.1. Design algorithm

An algorithm based on a lifting surface vortex model is used in order to design a screw propeller and the pre-swirl stator vanes. First of all, the number of stator blades, their length and angular positions as well as standard data for propeller design must be known in advance. These include the desired thrust force, number of blades, diameter, angular velocity, actual velocity field round the propeller and the design velocity of the ship. The main steps of the algorithm are shown in figure 1.

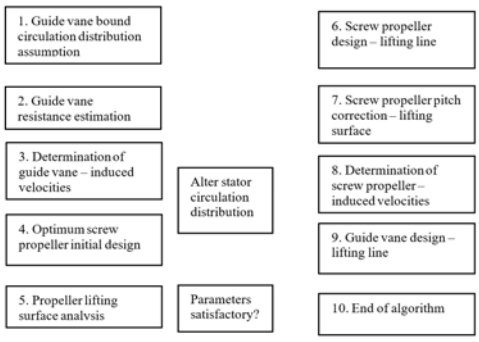

Figure 1. Block scheme of the screw propeller+guide vane design algorithm.

The main problem related to step 1 is to assume the bound circulation magnitudes and its distribution on each stator foil. The general idea here is to apply higher foil loading at positions where velocity field in propeller plane can by improved by the stator presence. From the lifting line theory, the lifting foil accelerates the velocity at its suction side and decelerates it at its pressure side, while total change in axial velocity is zero (if viscous effects are neglected). This effect can be used to make sharp velocity gradients smoother. The bound circulation distribution has important influence on the system operation as it influences directly the velocity field at the propeller location and the stator drag.

Further, the drag of the guide vanes in step 2 is estimated by using simplified formula [5]

$$D = 1.5\frac{L^2}{\pi\frac{1}{2}\rho V^2\lambda^2} \tag{1}$$

where D is a single stator foil resistance, L – the lifting force generated by this foil, ρ – water density, V is the design speed and λ is the respective foil length. This value is used later for initial evaluation of propulsor system efficiency. Equation (1) is based on the induced drag of lightly loaded hydrofoils with an elliptical loading distribution, operating in ideal fluid. It is increased here by a factor of 50% in order to take account for deviations from these assumptions, foils mutual interaction, viscous drag component, etc.

Lifting line representation of the stator foils is used to determine their induced velocities in step 3. These are calculated for the location of the propeller disc. Each foil is replaced with a set of straight line vortex segments with bound circulation variable spanwise. The geometry of the trailing vortex wake of the stator foils is calculated with an iterative scheme [5, 6]. What is more, the screw propeller presence is neglected during these calculations.

The optimal screw propeller design is prepared in step 4. This is achieved by means of the classical lifting line algorithm. The only difference is to take the stator-induced velocities into account, which is obviously not the case for the screw propeller operating alone. This propeller is then analysed further in step 5 by using a lifting surface software to estimate thrust and torque values at the design point. The next point is simply determination of the system efficiency. As the stator generates drag on itself it is included at this stage as the thrust decrease. It can be assumed, based upon CTO experience, that stator's drag is about 2-5% of the total resistance of the hull with operating propeller.

After that, the system efficiency is calculated according to the following formula

$$\eta = \frac{T - D}{2\pi nQ} \tag{2}$$

where η is the system efficiency, T – screw propeller thrust force, n – screw propeller rpm and Q is the screw propeller torque. If the calculated parameters are not satisfactory then the stator circulation distribution should be modified and all above-mentioned calculations repeated, starting from step 2. When the stator loading distribution, preserving satisfactory operation of the system, is found the design process can be continued.

The screw propeller geometry is prepared with more detail in step 6. First of all, the cavitation analysis is conducted with use of software whose description can be found in [1]. Moreover, the pitch distribution is corrected in step 7 by means of a lifting surface software. The propeller is analysed in a velocity field, taking both non-uniform wake field and stator-induced velocities into account. The hull presence alters the velocity field in which the propeller operates through its displacement and boundary layer. The velocity field measured past the hull without a propeller is referred to as a nominal wake. However, the propeller actually operates in the so called effective wake – the wake virtually experienced by the propeller. According to potential flow theory, the effective wake would be produced by a hull singularity and boundary layer system, altered by the propeller presence. What is more, the effective wake is merely a mathematical concept, being impossible to measure, because it takes no propeller induced velocities into account. Both concepts, i.e. nominal and effective wakes are well known in ship hydrodynamics. Many well established methods exist for recalculating measured nominal wakes into effective wakes [3]. In vortex calculations mean value of the effective wake is applied for each radial position. Further, it is assumed constant along the axial coordinate and taken as 'undisturbed' flow during the calculations. In viscous approach realised by means of CFD the effective wake concept is redundant, as the hull is directly present within the simulation.

The unit-span thrust force is calculated for each radii according to

$$\tau_i = \frac{T_i}{r_{i+1} - r_i} \tag{3}$$

where τ_i is the unit-span propeller blade thrust force at analysed radius i, T_i is the thrust force generated by the propeller blade bound vortices starting from analysed radius i and r_i are respective radii. Next, the unit-span thrust force values are compared with the ones determined within a screw propeller design process at respective radii. If these differ less than 1% over the whole propeller blade then the geometry is accepted. If, however, the difference is higher then the blade pitch angle is corrected at respective radius by means of the following formula

$$\Delta\varphi = \frac{\tau_D - \tau_C}{2\pi} \tag{4}$$

where φ is the screw propeller blade pitch angle, τ_D – demanded τ value at analysed radius and τ_C is the value calculated with the use of lifting surface model. After completing the screw propeller design, the geometry is finally analysed by using a lifting surface software. This time, however, not only the screw propeller dynamic characteristics are determined, but also its induced velocities in the stator plane. These serve as an input for a stator design in step 9. Since the propeller rotates with respect to its axis and the stator remains fixed, the average values for each radius are applied.

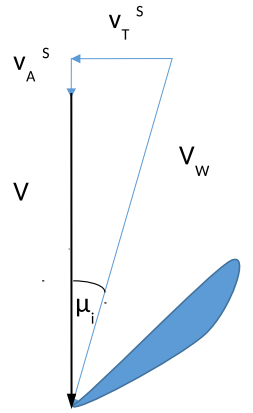

Figure 2. Velocity components on the guide vane foil element.

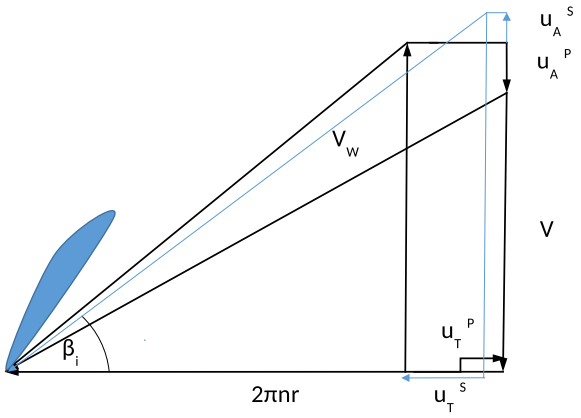

Figure 3. Velocity components on the propeller blade element.

Subsequently, the design of guide vane foils in step 9 is based on the algorithm that is very similar to the classical one used for the screw propellers in steps 4 and 6. Main differences are in the way of determination of local inflow angles, which are for a screw propeller given by

$$\beta_i = \arctan \frac{V + u_A^P - u_A^S}{2\pi nr - u_T^P + u_T^S} \tag{5}$$

where u is the velocity induced at the screw propeller disc, see figures 2 and 3. Subindex A means axial component and T denotes tangential. Superindex P denotes velocity induced by the propeller and S induced by the stator. Typically, the induced velocities u_T^P and u_A^S are negative. Furthermore, the velocities induced by the stator are taken as mean values for an individual radius. Respectively, the local inflow angle in case of the guide vane section profile is

$$\mu_i = \arctan \frac{v_T^S}{V + v_A^P + v_A^S} \tag{6}$$

where v is the velocity induced at the stator plane. Indices are the same as in the case of formula (5). Propeller-induced tangential velocity is not taken into account in equation (6) as due to the vortex theory its mean value is zero in any plane in front of it. Velocities induced by the propeller are taken as mean values for respective radius.

Moreover, as the guide vane foils have relatively high aspect ratio, no corrections for lifting surface are applied for determination of the angle of attack and profile camber. Pure lifting line model is used.

2.2. Designed system

The propulsor system consisting of a controllable pitch propeller CP753 and guide vanes ST002 was designed by means of the algorithm described above. The vessel used as an example was Nawigator XXI – training ship belonging to the the Szczecin Maritime University. The design assumptions for guide vanes + screw propeller propulsor are listed in table 1.

Table 1. Design input parameters.

Quantity	Symbol	Unit	Value
Total thrust	T	kN	125
Ship speed	V	knots	13
Number of propeller blades	Z	-	5
Propeller diameter	D	m	2.26
Rotation speed	n	rpm	259.7
Propeller delivered power	P_D	kW	1024
Number of guide vane foils	N	-	3
Guide vane foils length	λ	m	1.3

The propulsion system was manufactured and tested in the model scale (scale ratio 1:10). Further, the propulsor model mounted on the hull model is shown in figure 4. Self-propulsion test was conducted by means of continental method [14]. Full scale predictions was prepared according to the ITTC Recommendations and Guidelines [15].

Figure 4. Hull model equipped with propeller CP753 and stator ST002.

The most important design values of the designed screw propeller are the number of propeller blades $Z = 5$, propeller diameter $D = 2.26\,\mathrm{m}$, pitch ratio at radius 0.7 $P_{0.7}/D = 0.828$ and expanded area ratio EAR = 0.7592.

Guide vane design parameters are given for whole stator. Particular foils differ slightly among each other, however, these differences are so small that mean values provide sufficient information

about the guide vane. The guide vane design values are: angular interval $\Delta\gamma = 30°$, foil length $\lambda = 1.3\,\mathrm{m}$, mean angle of attack $\alpha_{\mathrm{mean}} = 18.91°$ and mean profile chord ratio $b_{\mathrm{mean}}/\lambda = 0.174$.

Full scale predictions based upon the model tests are in good agreement with design input. This can be inspected in table 2.

Table 2. Full scale prediction versus design input.

Quantity	Symbol	Unit	Des. value	Exp. value	Difference %
Propeller delivered power	P_D	kW	1024	1028	0.4
Propeller rate of revolution	n	rpm	259.7	265	2
Total thrust	T	N	125	126	0.8

Table 3. Model scale measurements in self-propulsion test.

Pt.	V_{M} m s^{-1}	n_{M} s^{-1}	T_{M} N	Q_{M} Nm
1	1.95	12.0	91.50	2.67
2	1.95	11.4	80.26	2.36
3	2.03	12.4	96.04	2.82
4	2.03	13.0	108.69	3.17
5	2.11	13.3	111.46	3.27
6	2.11	13.9	124.86	3.65
7	2.19	15.2	152.01	4.44
8	2.19	14.6	137.08	4.02
9	2.28	16.3	176.99	5.17
10	2.28	15.7	160.30	4.79

The self-propulsion test was conducted by means of continental method, which involves two measuring points for each tested ship speed. Model scale results are given in table 3. V_{M} is the ship model speed, n_{M} – propeller model rate of revolution, T_{M} – propeller model thrust and Q_{M} – propeller model torque.

3. Numerical methods

3.1. Lifting Surface method

The Lifting Surface software was developed as an auxiliary tool for the design process. It is based on well-known idea of replacing lifting foil with a set of discrete bound and free vortices, modelling loading effects and straight line source filaments, modelling foils finite thickness. The theoretical background of this method can be found in [1, 2, 4, 5, 6] or in the majority of papers on vortex lattice computations. Only simulation settings and assumptions are discussed here.

Both propeller blades and stator foils are discretised by 20 spanwise and 20 chordwise sections. Spanwise elements are concentrated around the tip by means of sine formula

$$r_i = r_0 + (1 - r_0) \sin \frac{\pi i}{2A - 2} \tag{7}$$

where r_i is a discrete radius i and A is the total number of discrete radii (in this case 20). Moreover, the chordwise spacing of discrete chordwise segments is achieved with constant steps both in the case of screw propeller blades and the guide vane foils. Analogical vortex grid was investigated in [7]. Consequently, the vortex grid convergence given in this reference is also representative for calculations with a pre-swirl stator.

The guide vanes vortex wake was assumed to remain flat and parallel to direction of ship advance speed during the simulation. It may appear to be significant simplification, however, only mean values of induced velocities are taken into account for propeller-stator interaction, as the propeller rotates, unlike the stator. According to well-known Stokes' theorem these mean values depend only on the calculation point radius, free vortices radial position and circulation. Stator-induced axial velocities in the propeller plane are much lower than tangential ones.

The screw propeller vortex wake is iteratively relaxed by a convective scheme. At each end of a free vortex discrete segment the total velocity is calculated – as a sum of undisturbed flow velocity, propeller-induced velocities and mean values of guide vane-induced velocities, proper for considered axial and radial position with respect to the guide vane. In order to preserve stability of a convective scheme the discrete vortex segment endpoints are not allowed to move more than $0.05D$. Moreover, the total velocity in each time step is taken as a weighted average of current (20%) and previous (80%) time steps. The time step value is taken such that propeller revolution angle is 5° within it. It takes around 15 iterations for a calculation point to get stable values of calculated propeller thrust and torque.

3.2. CFD

The Reynolds-Averaged Navier-Stokes approach to turbulence modelling is chosen to solve for averaged quantities. A closed system of equations for incompressible fluids can be formulated consisting of the continuity and Reynolds equation. Additional equations for the two-equation k-ω SST model [12, 16] are equation for transport of kinetic energy of velocity fluctuations k and equation for transport of turbulence frequency ω.

The system of equations is further discretised by means of the Finite Volume Method [10]. Convection terms and other diffusive terms take advantage of Gaussian integration. As for the discretised convection term, centroid variables are interpolated to the cell faces variables by second order limited linear upwind scheme. This make it possible to limit towards first-order upwind in regions of rapidly changing gradients. Diffusive terms involve surface normal gradients. An additional non-orthogonal correction is considered here to maintain second order accuracy for non-orthogonal meshes. The same applies to Laplacian schemes. Moreover, gradient terms, such as pressure gradient, are discretised by means of Gaussian integration. Central differencing is used here in order to interpolate values from cell centres to face centres. Additionally, cell limiting is also introduced in order to improve boundedness and stability [13].

The discretised governing equations are solved by means of the open source software for CFD OpenFOAM [13]. The SIMPLE algorithm is used in order to solve pressure-velocity coupling. The pressure equation is solved by means of GAMG solver with DIC smoother [13]. For the velocity fields as well as turbulent quantities standard solver using a Gauss-Seidel smoother is used. Additionally, under-relaxation factors are used in order to improve stability of a solution.

The flow domain, shown in figure 5, consists of two parts, namely the rotating propeller and the steady hull (figure 6) inside a towing tank. Breadth and depth of the tank correspond to the real dimensions of the Ship Design and Research Centre towing tank, which dimensions length × breadth × depth are 270 × 12 × 6 m respectively. Both domains are discretised separately and merged by means of the arbitrary mesh interfaces. Computational grids can be classified as Cartesian. The merged mesh consists of 8 961 314 nodes and 8 408 464 volumes where 7 536 421 are hexahedra. The maximal y^+ value on the blades does not exceed 5. Figure 7 displays mesh convergence by showing the influence of number of nodes on the T and Q. It can be seen that

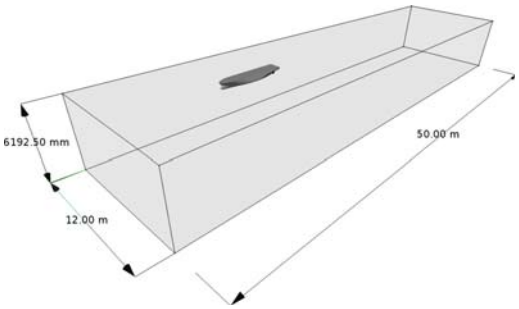

Figure 5. Flow domain.

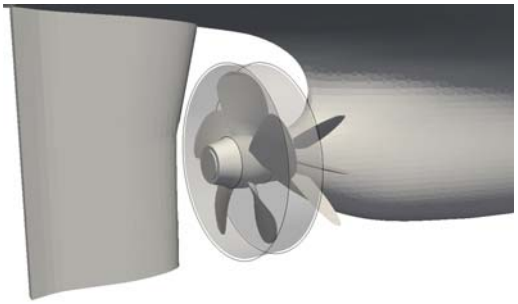

Figure 6. Rotating propeller and steady hull.

increasing the number of the mesh nodes above 9×10^6 has negligible effects on T and Q in particular. Mesh convergence test was conducted for a single point 5 in table 3.

The main boundary conditions include inlet, outlet, walls (side and bottom walls, hull, rudder and shaft) and top symmetry surface. As for the inlet, the fixed velocity perpendicular to inlet surface together with zero normal gradient pressure is specified. Low turbulence intensity case is also assumed. Furthermore, the constant pressure distribution is assumed at the outlet accompanied with zero gradient velocity. This can be justified simply because the outlet surface is located far from the propeller. The impermeability and adhesion condition are specified on the walls, i.e. the no-slip condition. The scalable wall function approach is used in the near wall region. Finally, the so called cyclic arbitrary mesh interface is considered allowing for coupling between stationary domain and rotating propeller. Most importantly, a steady state approach is used also referred to as a multiple reference frame simulation. This saves computational time considerably in comparison with the full transient rotor-stator interaction.

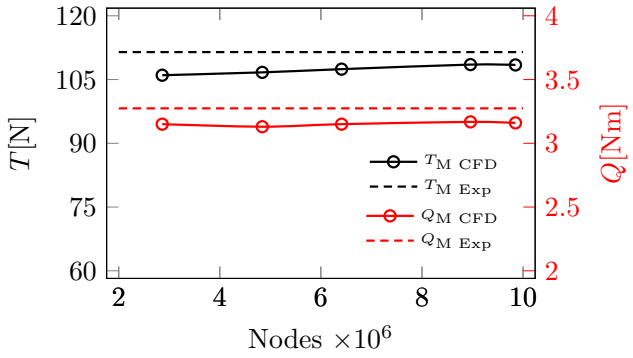

Figure 7. Mesh convergence.

4. Results

The model scale measurements were reproduced by two numerical methods, i.e. lifting surface analysis (in-house code) and CFD (OpenFOAM). The model scale speed V_M and propeller rate of revolution n_M were regarded as input values and the propeller model thrust T_M and torque Q_M were calculated during the simulations. Results are presented in table 4 where 'Exp' denotes experimental value, 'LS' Lifting Surface method results and 'CFD' results from CFD calculations. The relative error is denoted here as ΔT or ΔQ.

It can be easily seen that in general the error of CFD predictions is notably lower and more stable than in Lifting Surface Method results. On the other hand a single calculation point with LS method requires around 30 minutes (quad-core processor i5-4590, 3.30 GHz – 1 core engaged)

while CFD requires 180-200 minutes (six-core processor i7-6850K, 3.60 GHz – 6 cores engaged). Keeping in mind that the six-core i7 processor is several times faster than quad-core i5, it becomes obvious that CFD approach is about 20 times slower. This makes the vortex methods still attractive since it is capable of providing accuracy sufficient for practical application.

Table 4. Model scale calculations in self-propulsion test.

Pt.	$T_{\mathrm{M\,Exp}}$ N	$T_{\mathrm{M\,LS}}$ N	$T_{\mathrm{M\,CFD}}$ N	$\Delta T_{\mathrm{M\,LS}}$ %	$\Delta T_{\mathrm{M\,CFD}}$ %	$Q_{\mathrm{M\,Exp}}$ Nm	$Q_{\mathrm{M\,LF}}$ Nm	$Q_{\mathrm{M\,CFD}}$ Nm	$\Delta Q_{\mathrm{M\,LS}}$ %	$\Delta Q_{\mathrm{M\,CFD}}$ %
1	91.50	87.53	87.10	4.34	4.80	2.67	2.67	2.55	0.19	4.67
2	80.26	82.96	75.90	3.36	5.42	2.36	2.48	2.23	4.95	5.48
3	96.04	96.99	92.51	0.99	3.67	2.82	2.94	2.70	4.95	4.01
4	108.69	111.10	104.87	2.22	3.50	3.17	3.31	3.05	4.95	3.71
5	111.46	114.95	108.53	3.13	2.63	3.27	3.13	3.16	4.40	3.22
6	124.86	129.24	121.94	3.51	2.33	3.65	3.85	3.54	5.54	2.84
7	152.01	159.84	150.43	5.15	1.03	4.44	4.74	4.35	6.68	2.06
8	137.08	143.75	135.47	4.87	1.17	4.02	4.28	3.93	6.47	2.16
9	176.99	156.21	176.30	11.74	0.38	5.17	4.78	5.08	7.47	1.55
10	160.30	151.37	160.02	5.57	0.17	4.70	4.56	4.62	2.94	1.45

Acknowledgments
The experimental results and design algorithm presented and discussed in the paper were developed within the CTO Internal Research Found.

References

[1] Bugalski T and Szantyr J 2014 Numerical Analysis of the Unsteady Propeller Performance in the Ship Wake Modified By Different Wake Improvement Devices, *Polish Maritime Research* 3(83), 32
[2] Greeley D and Kerwin J 1982 Numerical Methods for Propeller Design and Analysis in Steady Flow, *Transactions of Society of Naval Architects & Marine Engineers* **90**, 415
[3] Jarzyna H 1993 Wzajemne oddzialywanie kadluba i pednika statku (Wroclaw: Ossolineum)
[4] Kerwin J, Coney W and Hsin C 1988 Hydrodynamic Aspects of Propeller/Stator Design, *Propellers' 88 Symposium 5th (Virginia Beach)*
[5] Król P and Bugalski T 2017 Application of vortex flow model in propeller-stator system design and analysis, *Polish Maritime Research* **1**(97) 35
[6] Król P, Bugalski T and Wawrzusiszyn M 2017 Development of numerical methods for marine propeller – pre-swirl stator system design and analysis *Fifth International Symposium on Marine Propulsion (Espoo)*
[7] Król P and Tesch K 2018 Experimental and numerical validation of the improved vortex method applied to CP745 marine propeller model, *Polish Maritime Research* **2**(98) 56
[8] Kim J, Choi J, Choi B, Chung S and Seo H 2015 Development of energy-saving devices for a full slow-speed ship through improving propulsion performance *International Journal of Naval Architecture and Ocean Engineering* **7**(2) 390
[9] Chen K, He W, Qin J and Wang L 2013 On the Design of Energy Saving Shaft Bracket for a Twin Screw Vessel *2013 Proceedings of the Twenty-third International Offshore and Polar Engineering Conference (Anchorage)*
[10] Ferziger J H and Perić M 2002 Computational methods for fluid dynamics (Berlin: Springer-Verlag)
[11] Kim M, Chun H and Kang Y 2004 Design and Experimental Study on a New Concept of Preswirl Stator as an Efficient Energy-Saving Device for Slow Speed Full Body Ship *Transactions-Society of Naval Architects and Marine Engineers* **112** 111
[12] Menter F R 1994 Two-equations eddy-viscosity turbulence models for engineering applications *AIAA-Journal* **32**(8)
[13] OpenFOAM user guide 2015, OpenFOAM Foundation Ltd.

[14] Propulsion Committee of the 28th ITTC Propulsion/Bollard Pull Test ITTC Quality System Manual Recommended Procedures and Guidelines 2017
[15] Propulsion Committee of the 28th ITTC 1978 ITTC Performance Prediction Method ITTC Quality System Manual Recommended Procedures and Guidelines 2017
[16] Wilcox D C 1994 Turbulence modeling for CFD (California: DCW Industries)